Clinical & Translational Immunology

Australian and New Zealand Society for Immunology Inc.

Clinical & Translational Immunology 2024; e1488. doi: 10.1002/cti2.1488
www.wileyonlinelibrary.com/journal/cti

SHORT COMMUNICATION

Whole transcriptome profiling of placental pathobiology in SARS-CoV-2 pregnancies identifies placental dysfunction signatures

Nataly Stylianou[1,a], Ismail Sebina[2,a], Nicholas Matigian[3], James Monkman[2], Hadeel Doehler[1], Joan Röhl[4], Mark Allenby[5], Andy Nam[6], Liuliu Pan[6], Anja Rockstroh[1], Habib Sadeghirad[2], Kimberly Chung[2], Thais Sobanski[1], Ken O'Byrne[7], Ana Clara Simoes Florido Almeida[8], Patricia Zadorosnei Rebutini[8], Cleber Machado-Souza[9], Emanuele Therezinha Schueda Stonoga[10], Majid E Warkiani[11], Carlos Salomon[12], Kirsty Short[13], Lana McClements[11], Lucia de Noronha[8], Ruby Huang[14], Gabrielle T Belz[2], Fernando Souza-Fonseca-Guimaraes[2], Vicki Clifton[15] & Arutha Kulasinghe[2]

[1]Australian Prostate Cancer Research Centre – Queensland, Centre for Genomics and Personalised Health, School of Biomedical Sciences, Faculty of Health, Queensland University of Technology, Brisbane, QLD, Australia
[2]Frazer Institute, Faculty of Medicine, The University of Queensland, Brisbane, QLD, Australia
[3]QCIF Bioinformatics, St Lucia, QLD, Australia
[4]Faculty of Health Sciences and Medicine, Bond University, Robina, QLD, Australia
[5]BioMimetic Systems Engineering Lab, School of Chemical Engineering, University of Queensland (UQ), St Lucia, QLD, Australia
[6]Nanostring Technologies, Inc., Seattle, WA, USA
[7]Princess Alexandra Hospital, Woolloongabba, QLD, Australia
[8]Postgraduate Program of Health Sciences, School of Medicine, Pontifícia Universidade Católica do Paraná´ –PUCPR, Curitiba, Brazil
[9]Postgraduate Program in Biotechnology Applied in Health of Children and Adolescent, Instituto de Pesquisa Pelé Pequeno Príncipe, Faculdades Pequeno Príncipe, Curitiba, Brazil
[10]Department of Medical Pathology, Clinical Hospital, Universidade Federal do Paraná´ –UFPR, Curitiba, Brazil
[11]School of Life Sciences & Institute for Biomedical Materials and Devices, Faculty of Science, University of Technology Sydney, Sydney, NSW, Australia
[12]Exosome Biology Laboratory, Centre for Clinical Diagnostics, University of Queensland Centre for Clinical Research, Royal Brisbane and Women's Hospital, Faculty of Medicine, The University of Queensland, Brisbane, QLD, Australia
[13]School of Chemistry and Molecular Biosciences, Faculty of Science, The University of Queensland, St Lucia, QLD, Australia
[14]School of Medicine, College of Medicine, National Taiwan University, Taipei, Taiwan
[15]Mater Medical Research Institute, University of Queensland, Brisbane, QLD, Australia

Correspondence
A Kulasinghe, Frazer Institute, Faculty of Medicine, The University of Queensland, 37 Kent Street, Woolloongabba, QLD 4012, Australia.
E-mail: arutha.kulasinghe@uq.edu.au

[a] Equal contributors.

Received 22 November 2023;
Revised 10 and 17 January 2024;
Accepted 18 January 2024

doi: 10.1002/cti2.1488

Clinical & Translational Immunology 2024; **13**: e1488

Abstract

Objectives. Severe Acute Respiratory Syndrome Coronavirus 2 (SARS-CoV-2) virus infection in pregnancy is associated with higher incidence of placental dysfunction, referred to by a few studies as a 'preeclampsia-like syndrome'. However, the mechanisms underpinning SARS-CoV-2-induced placental malfunction are still unclear. Here, we investigated whether the transcriptional architecture of the placenta is altered in response to SARS-CoV-2 infection. **Methods.** We utilised whole-transcriptome, digital spatial profiling, to examine gene expression patterns in placental tissues from participants who contracted SARS-CoV-2 in the third trimester of their pregnancy (n = 7) and those collected prior to the start of the coronavirus disease 2019 (COVID-19) pandemic (n = 9). **Results.** Through comprehensive spatial transcriptomic analyses of the trophoblast and villous core stromal cell subpopulations in the placenta, we

identified SARS-CoV-2 to promote signatures associated with hypoxia and placental dysfunction. Notably, genes associated with vasodilation (*NOS3*), oxidative stress (*GDF15*, *CRH*) and preeclampsia (*FLT1*, *EGFR*, *KISS1*, *PAPPA2*) were enriched with SARS-CoV-2. Pathways related to increased nutrient uptake, vascular tension, hypertension and inflammation were also enriched in SARS-CoV-2 samples compared to uninfected controls. **Conclusions.** Our findings demonstrate the utility of spatially resolved transcriptomic analysis in defining the underlying pathogenic mechanisms of SARS-CoV-2 in pregnancy, particularly its role in placental dysfunction. Furthermore, this study highlights the significance of digital spatial profiling in mapping the intricate crosstalk between trophoblasts and villous core stromal cells, thus shedding light on pathways associated with placental dysfunction in pregnancies with SARS-CoV-2 infection.

Keywords: COVID-19, digital spatial profiling, gene expression profiling, placental dysfunction, SARS-CoV-2, trophoblasts

INTRODUCTION

Viral infections in pregnancy can disrupt placental function and predispose pregnancy complications, including late-onset preeclampsia, preterm birth, stillbirth and intrauterine foetal demise.[1–4] Recent studies have revealed that pregnant women who contract Severe Acute Respiratory Syndrome Coronavirus 2 (SARS-CoV-2, which causes coronavirus disease 2019 [COVID-19]), can experience placental dysfunction and what has been referred to as 'preeclampsia-like syndrome'.[5–10] Placental tissues from COVID-19 patients exhibit increased vasculopathy and inflammation, which are characteristic pathological features of preeclampsia.[11] Moreover, clinical manifestations observed in COVID-19 patients, such as COVID-19-associated hypoxia, hypertension, endothelial dysfunction, kidney disease, thrombocytopenia and liver injury, overlap with those observed in preeclampsia.[5,12] However, mechanisms through which SARS-CoV-2 infection predisposes pregnancies to these preeclampsia-like pathological features are largely unclear.

The placenta is vital for foetal development and growth throughout gestation as it is a functional interface between the mother and foetus.[13] This interface comprises various anatomically distinct sites, including the decidua basalis, where maternal immune cells and decidual stromal cells interact with foetal extravillous trophoblasts.[14] The maternal–foetal interface also consists of the placental intervillous space, where maternal immune cells interact with foetal syncytiotrophoblasts, and the boundary between the parietalis and the chorion laeve in the chorioamniotic membranes.[14] Other cell types within this interface, such as villous cytotrophoblasts, column cytotrophoblasts, fibroblasts, endothelial cells and Hofbauer cells, contribute to nutrient and waste exchange, hormone production, protection from pathogens, and maternal immune responses essential for foetal development.[13,14] Whether SARS-CoV-2 infection modifies the transcriptomic architecture and functional characteristics of different cell types within these distinct placental sites is still unclear.

In this study, we utilised digital spatial whole-transcriptomic analysis of human placental tissue to delineate molecular pathways associated with SARS-CoV-2 infection-induced placental pathology in pregnancy. Specifically, we focused our analysis on defining the distinct transcriptional profiles of trophoblasts and villous core stromal cell populations (the latter including endothelial, fibroblast and immune cells), in the context of SARS-CoV-2 infection. We identified several pivotal pathways that underlie the development of a 'preeclampsia-like syndrome' associated with SARS-CoV-2 infection in pregnancy.

RESULTS

Characterisation of patient demographics and histopathology in collected placentae

Tissue microarrays were constructed using placental cores that were collected immediately

after birth from unvaccinated participants who had tested positive within 15 days prior to delivery (Alpha strain, April 2020, $n = 7$), and unvaccinated participants who were negative for SARS-CoV-2 throughout their pregnancy (n = 9; Table 1). There were no significant differences in maternal age, gestational age, foetal weight, placental weight, foetal sex, foetal outcome and delivery method, between the two groups (Supplementary table 1). Comorbidities were matched as closely as possible between the SARS-CoV-2 and control groups.

No SARS-CoV-2 viral load was detected in the placental cores from the SARS-CoV-2 infected group through examination by RNAscope of the SARS-CoV-2 spike mRNA (data not shown). With the aid of a trained placental pathologist, an area featuring an anchoring villus, and an area featuring a cluster of terminal villi, were designated as two areas of interest (AOI) within each placental core (Figure 1a). AOIs were immunofluorescently stained with PanCK to identify trophoblast populations, and vimentin to identify stromal populations (i.e. fibroblasts, endothelial cells). Transcriptional expression was collected separately for PanCK positive and separately for vimentin positive cells within each AOI using the Whole Transcriptome Atlas kit (Nanostring; Figure 1a). Subsequent cell deconvolution was performed to assess the purity of each collection (Figure 1b). As expected, transcriptional expression from PanCK positive regions within the AOIs had high proportion of trophoblast populations, compared to vimentin positive regions that had higher proportions of fibroblast and endothelial cells (Figure 1b–f). As a result of the overlapping nature of cells, all samples captured a proportion of immune cell types (macrophages, monocytes, Hofbauer cells), except for the PanCK positive regions that displaying a proportion of granulocytes that was absent from the vimentin positive regions within the AOIs (Figure 1b and g–j). SARS-CoV-2 infection did not significantly alter the transcriptional proportion of any cell type assessed than in controls (Figure 1b–j). In subsequent analyses, the PanCK positive regions within the AOIs will be referred to as 'Trophoblasts' and the vimentin positive regions will be referred to as 'Villous Core Stroma' compartments, because of the predominant enriched cell type they represent.

SARS-CoV-2 infection related pathways enriched in the placenta despite absence of detectable viral particles

Unsupervised clustering of the normalised gene counts by principal component analysis showed that SARS-CoV-2 samples clustered separately to control samples in dimension 1, and further by phenotype in dimension 2, supporting that infection with SARS-CoV-2 markedly alters the transcriptional profiles of the trophoblast and villous core stromal cell populations (Figure 2a and b). Notably, there was very high overlap of genes differentially expressed between the anchoring and the terminal villi; for instance, trophoblasts at the anchoring villi had 1791 differentially expressed genes versus 493 at the terminal villi, with 402 genes in common between them (82% overlap; Supplementary table 2, Figure 2c). Similarly, the villous core stromal cells at the anchoring villi had 1139 differentially expressed genes versus 601 at the terminal villi, with 459 genes in common between them (76% overlap; Supplementary table 2, Figure 2c). As expected, there was minimal overlap in differential gene expression between the trophoblasts and villous core stromal compartments, which highlights their distinct cell phenotypes (Figure 2c).

Despite the SARS-CoV-2 samples showing undetectable SARS-CoV-2 by RNA-scope, transcriptional profiling showed positive enrichment of SARS-CoV-2 related pathways in the SARS-CoV-2 samples, such as 'SARS_COV_2_INFECTION', and 'SARS_COV_2_HOST_INTERACTIONS' from the Reactome database, as well as the Interferon Alpha Response pathway from the Hallmark database, which is a first-line immune response pathway that has been associated with SARS-CoV-2 infection (Figure 2d–f).[15] These pathways were supported by increased expression of genes that have been associated with SARS-CoV-2, such as the inflammatory marker *IFI16*,[16] disease progression marker *IFI27*,[17] disease prognosticator *B2M*,[18] activation of Janus Kinases (i.e. *JAK1*), and expression of *STAT3*[19] (Figure 2g–j). Notably, gene expression for these markers was elevated predominantly in the villous core stromal cell compartment, presumably stemming from the immune subpopulation within the stroma. Indeed, specific analysis of the villus core stromal compartment revealed enrichment of several immune-related pathways from the Hallmarks database such as IL6/JAK/STAT3 signalling, IL2/STAT5 signalling, TNF-alpha signalling, inflammatory

Table 1. Clinical information of the SARS-CoV-2 and control cohorts

Patient De-ID	Group	Sample Code	Maternal Age	Gestational Age	Comorbidities	SARS-CoV-2 Symptoms/ Severity	Foetal Sex	Foetal Outcome	Delivery Method	Foetal Weight (g)	Placental Weight (g)	Macroscopic Observations
20–3594	SARS-CoV-2	2	26	30–35	Hypothyroidism and hypertensive disorder in pregnancy	+/+	Male	Preterm	na	2450	448	Infarcts and intervillous thrombosis (< 5%)
20–3561	SARS-CoV-2	4	38	25–30	Hypothyroidism	+/+	Female	Preterm	C-section	na	245	–
20–3744	SARS-CoV-2	8	29	30–35	Gestational diabetes, bipolar disorder, hypothyroidism and syphilis (treated)	+/–	Female	Preterm	C-section	na	412	Infarcts (< 5%)
20–5105	SARS-CoV-2	12	29	35–40	None	–	Female	Term	C-section	2960	462	–
20–3369	SARS-CoV-2	13	29	35–40	Gestational diabetes and hyperthyroidism	+/–	Female	Term	Assisted Vaginal	2600	358	Retroplacental and marginal hematoma, infarcts (< 5%)
20–5869	SARS-CoV-2	18	27	35–40	None	+/–	Male	Term	C-section	2345	370	–
20–2916	SARS-CoV-2	22	24	35–40	None	–	Female	Term	Assisted Vaginal	3030	650	–
16–7859	Control	1	20	30–35	Hypothyroidism		Male	Preterm	C-section	1180	270	Placental hypoplasia
18–13 016	Control	3	23	35–40	Hypothyroidism and hypertension		Female	Preterm	Assisted Vaginal	2223	498	–
16–8315	Control	5	18	40–45	Obesity		Female	Term	Assisted Vaginal	3810	514	–
18–4906	Control	9	20	30–35	None		Male	Preterm	Assisted Vaginal	1205	248	–
18–14 057	Control	10	42	30–35	Diabetes, hypertension, bipolar disorder		Male	Preterm	C-section	1650	243	Placental hypoplasia
16–7599	Control	11	25	35–40	Gestational diabetes		Male	Term	C-section	3460	480	–
16–3340	Control	15	39	35–40	None		Female	Term	C-section	3005	395	–
18–9951	Control	16	24	35–40	None		Male	Term	C-section	3690	574	–
16–6144	Control	19	29	35–40	None		Male	Term	C-section	3345	394	–

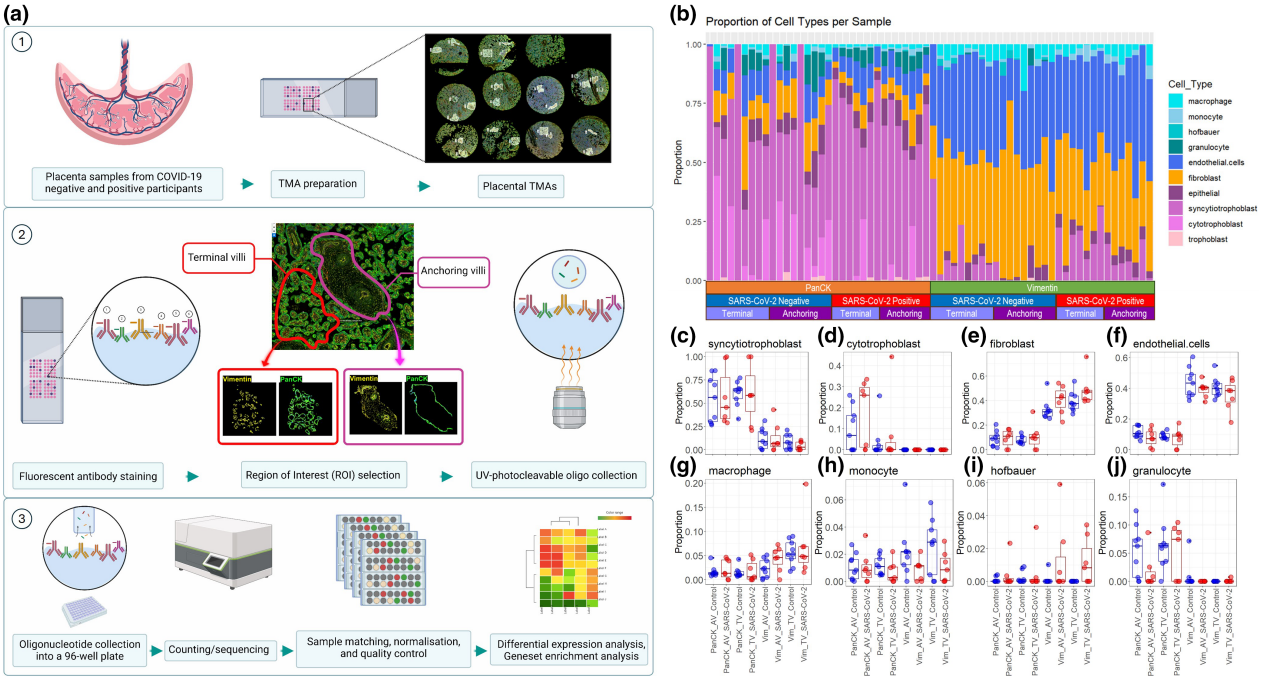

Figure 1. Study design and cell deconvolution. **(a)** (1) Placental cores collected at delivery from the SARS-CoV-2 (n = 7) and control (n = 9) groups were assembled into tissue microarray slides (TMAs). (2) TMAs were stained with fluorescent markers to differentiate cell types within anchoring (pink outline) and terminal villi (red outline). Barcodes were cleaved and collected from each region of interest by UV light. (3) Cleaved barcodes were sequenced and counted using an Illumina® sequencer in preparation for transcriptomic analysis. Data were normalised before downstream differential expression analysis. **(b)** Transcriptional cell deconvolution map. **(c–j)** Box-plots of indicated cell type proportions from 1b. No significant differences were detected between the SARS-CoV-2 group (n = 7) and control group (n = 9) by the unpaired t-test. AV, anchoring villi; TV, terminal villi.

response and complement pathways (Figure 3a), supporting that the immune cells within the placental villi are actively responding to SARS-CoV-2 infection.

SARS-CoV-2 infection enriches hypoxia and placental dysfunction pathways

Pathway enrichment analysis of the genes differentially expressed in response to SARS-CoV-2 infection, revealed pathways related to placental dysfunction, in both the trophoblast and villous core stromal compartments. For instance, hypoxia and oxidative phosphorylation pathways were enriched in the villous core stroma (Figure 3a), both of which have been previously linked with placental dysfunction and increased incidence of developing preeclampsia.[20] Hypoxia triggers TGF-β signalling and angiogenesis,[21] and both TGF-β signalling and angiogenesis related pathways were enriched in the villous core stroma in response to SARS-CoV-2 infection (Figure 3b). Furthermore, pathways related to haemorrhage were upregulated and pathways related to vascular tension, such as hyperaldosteronin/renin pathways, acetylcholine channels and olfactory receptors, were downregulated in the villous core stroma (Figure 3b). Trophoblast cells exhibited enrichment of pathways related to nitric oxide production (Figure 3c), which is a potent vasodilator.[22] Conversely, pathways related to calcium import[23] and vasoconstriction were downregulated in trophoblasts (Figure 3c), supporting the notion that the placenta actively reduces vascular tension during SARS-CoV-2 infection. In parallel, trophoblasts showed an increase in cell–cell adherence, communication and transmembrane amino acid transport, including MTORC1 signalling,[24] suggesting that nutritional uptake to the foetus is enhanced in response to SARS-CoV-2 infection (Figure 3a and c). Further, pathways related to allograft rejection and MHC molecules were decreased, suggestive of a defensive mechanism by the trophoblast layer to protect gestation (Figure 3a and c).

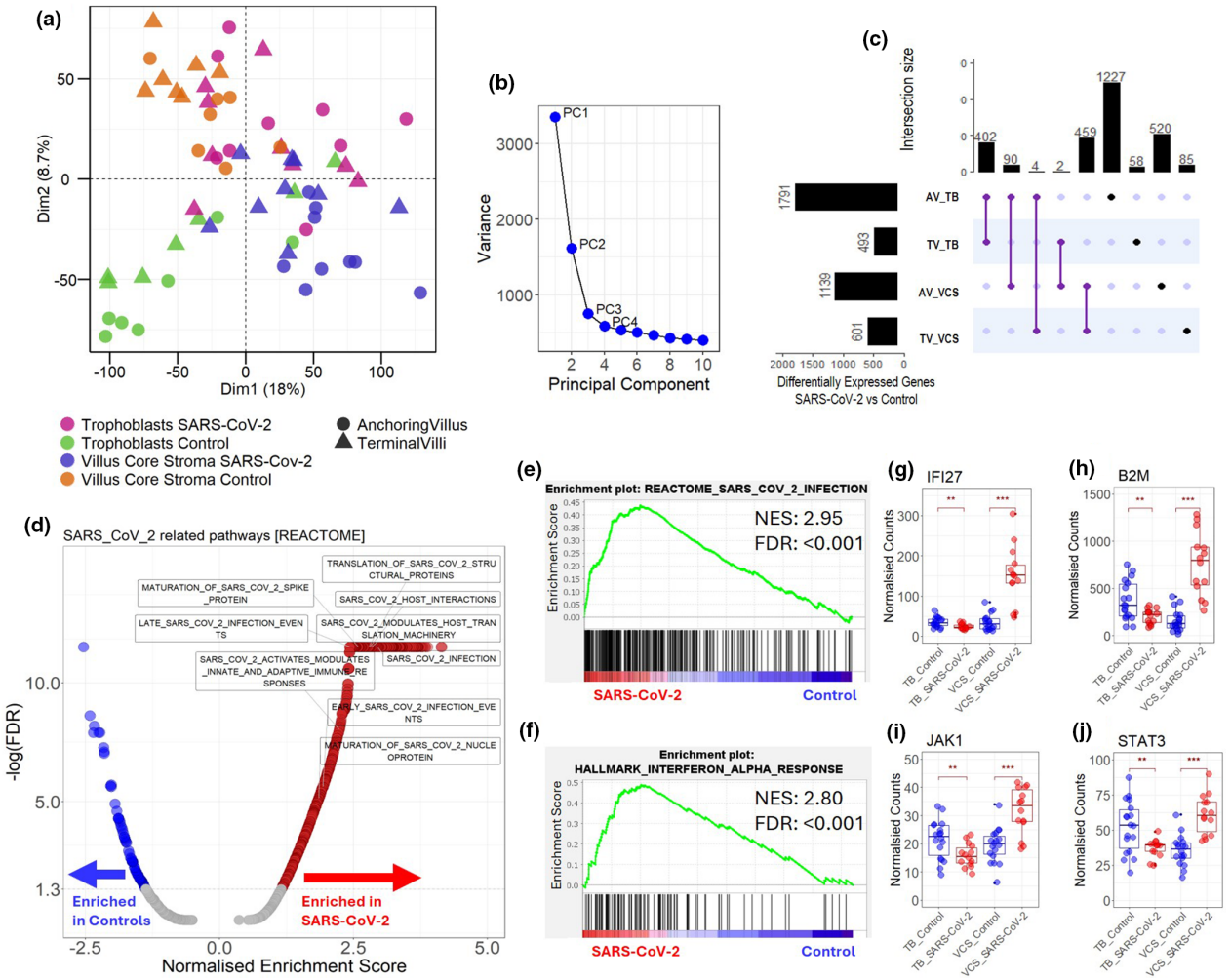

Figure 2. Enrichment of SARS-CoV-2 related pathways. **(a)** Principal component analysis of normalised gene counts from trophoblasts and villous core stromal compartments from SARS-CoV-2 (n = 7) and control (n = 9) groups at the anchoring or terminal villi (AV; TV). **(b)** Principal component dimensions. **(c)** Upset plot of differential gene expression in trophoblasts and villous core stromal compartments from the AV and TV in response to SARS-CoV-2 infection. The bar charts on the left indicate the total number of differentially expressed genes for the indicated sample group and the bar charts on the top show the gene overlap for the comparisons indicated by the purple lines. Black dots denote differentially expressed genes that are unique for the indicated sample group. Fold change ±1.5, P-value ≤ 0.05, FDR < 0.05. **(d)** Enrichment of significant SARS-CoV-2 related pathways from the Reactome database, in the SARS-CoV-2 and control samples. Blue: significantly negatively enriched, red: significantly positively enriched, grey: not significant. The full list of enriched pathways from the Reactome database can be found in Supplementary tables 3 and 4. **(e)** Gene set enrichment analysis (GSEA) plot of the SARS_COV_2_INFECTION pathway from the Reactome database and **(f)** INTERFERON_ALPHA_RESPONSE from the Hallmark database, in SARS-CoV-2 samples versus controls. **(g–j)** Normalised expression counts of IFI27, B2M, JAK1 and STAT3 genes, in trophoblast (TB) or villous core stroma (VCS) compartments from the SARS-CoV-2 (n = 7) and control samples (n = 9). ** P-value < 0.01, *** P-value < 0.001.

Markers associated with preeclampsia are elevated with SARS-CoV-2

Placentae from the SARS-CoV-2 group showed several markers that have been previously associated with hypoxia and placental dysfunction. For instance, the hypoxia and preeclampsia associated markers Fms Related Receptor Tyrosine Kinase 1 (*FLT1)*, *FLT4*, epidermal growth factor receptor (*EGFR)* and pappalysin-2 (*PAPPA2*) were increased in trophoblasts from the SARS-CoV-2 group (Figure 3e–i).[25–28] Additionally, markers associated with placental dysfunction and oxidative stress such as Nitric oxide synthase 3 (*NOS3*),[29] corticotrophin-releasing hormone (*CRH*),[30] kisspeptin 1 (*KISS1*),[31] Growth Differentiation Factor 15 (*GDF15*),[32] and tissue factor pathway inhibitor 2 (*TFPI-2*),[33] were also elevated in

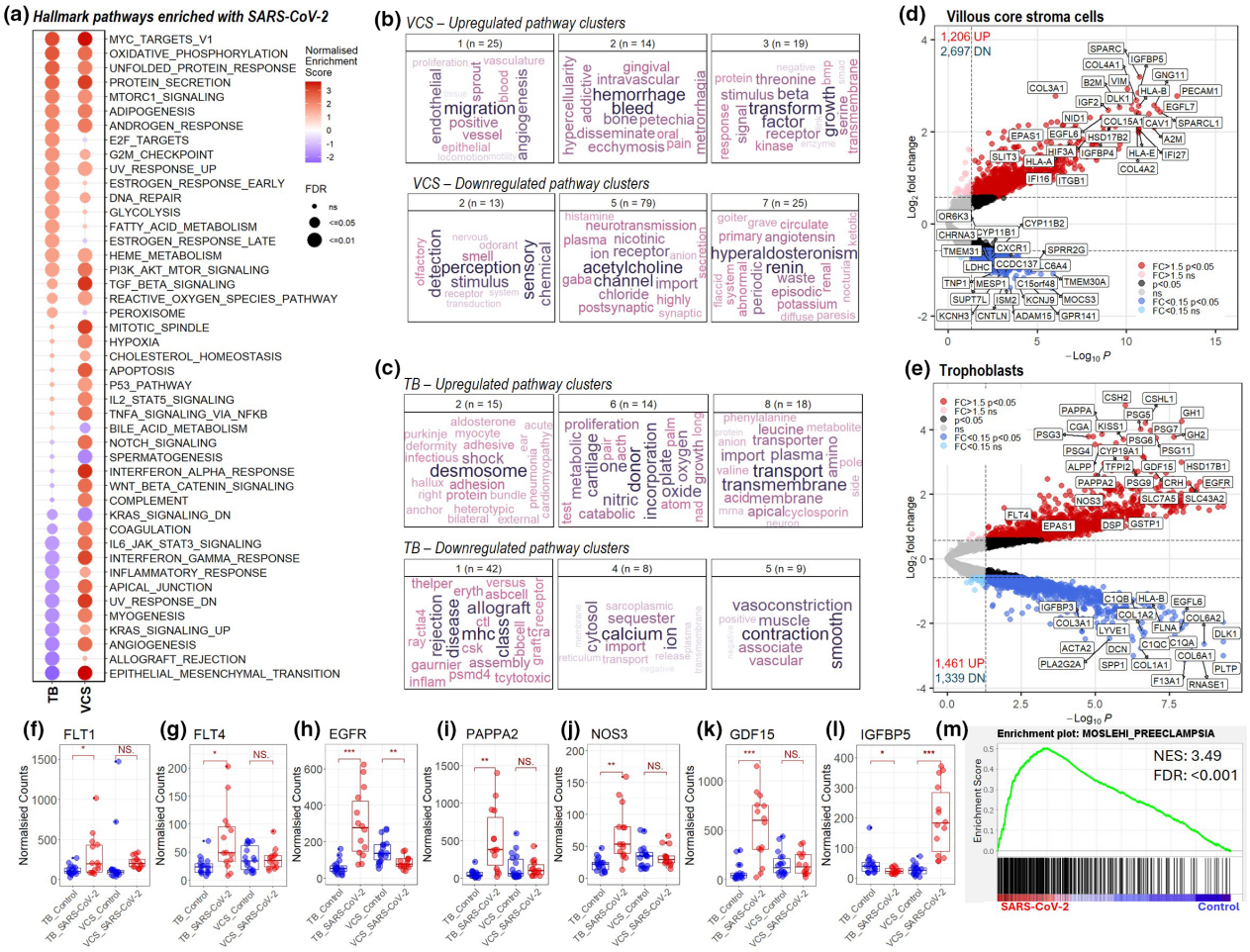

Figure 3. Enrichment of placental dysfunction pathways with SARS-CoV-2. **(a)** Differentially enriched pathways form the Hallmarks database in trophoblasts (TB) and villous core stromal (VCS) compartments in SARS-CoV-2 (n = 7) versus control group (n = 9). Colour gradient refers to the normalised enrichment score. **(b)** Enriched gene ontology biological processes (GO-BP) pathway clusters from the Molecular Signatures Database (MSigDb) generated using vissE, in the VCS and **(c)** TB. Top row depicts upregulated pathways, bottom row depicts downregulated pathways. **(d)** Volcano plot of gene expression from VCS or **(e)** TB in response to SARS-CoV-2 infection. Fold change (FC) ± 1.5, P-value ≤ 0.05, FDR < 0.05, the full list of differentially expressed genes can be found in Supplementary table 5. **(f–l)** Normalised expression counts of indicated genes in TB or VCS compartments from the SARS-CoV-2 (n = 7) and control samples (n = 9). *P-value < 0.05, **P-value < 0.01; ***P-value < 0.001; NS, not significant. **(m)** Gene set enrichment analysis (GSEA) plot of the preeclampsia signature generated by Moslehi *et al.*, in SARS-CoV-2 samples versus controls.

the trophoblasts from the SARS-CoV-2 group (Figure 3e, j, k). Transforming growth factor b1 (*TGFβ-1*), and the PAPP-A2 substrates *IGFBP4/5* (Figure 3d and l), were also elevated in the villous core stroma, both markers associated with increased preeclampsia risk.[21,34]

Given that a number of these pathways and genes are associated with preeclampsia, as well as several recent studies reporting SARS-CoV-2 in predisposing pregnant individuals to preeclampsia,[5–10] we next assessed the enrichment of a preeclampsia-specific gene set generated from published patient cohorts.[35] The gene set was generated by Moslehi *et al.*,[35] where they found 419 genes to be common between four studies examining preeclampsia versus healthy pregnancies. These 419 genes are involved in pathways relevant to preeclampsia, such as oxidative stress, hypoxia and immune response.[35–37] In our data, this preeclampsia signature was positively enriched in patient samples from the SARS-CoV-2 group (NES 3.49, FDR < 0.001; Figure 3m), which aligns with the positive enrichment of hypoxia, immune and oxidative stress, related pathways we observed in our studies (Figure 3a).

DISCUSSION

Using digital spatial profiling, we quantified the expression of key markers within distinct cellular compartments of the placenta, providing a detailed picture of the molecular changes occurring in response to SARS-CoV-2 infection. Although our study is limited by its relatively small cohort, cross-sectional nature and low availability of clinical data, it offers valuable insights into the interplay between trophoblasts and the cells within the villous core stroma in the placenta and how this relationship is influenced by SARS-CoV-2 infection. Close examination of the transcriptional alterations occurring in the placental trophoblast and villous core stroma in response to SARS-CoV-2, revealed a notable number of genes that are enriched in biological pathways previously associated with placental dysfunction.

Trophoblasts from the SARS-CoV-2-infected group had significantly higher levels of *NOS3* compared to the control group (Figure 3j). The upregulation of NOS3 is associated with increased endogenous production of the vasodilator nitric oxide, as a response to altered vascular reactivity, endothelial dysfunction and hypertension.[22,38] Interestingly, NOS has been previously found to be highly upregulated to supraphysiological levels in animal models of infection-mediated inflammation during pregnancy, leading researchers to hypothesise that increased NOS may play a role in placental inflammation.[39–41] In response to increased NOS expression by the trophoblasts, the villous core stroma showed elevated expression in biological pathways related to systemic pressure and vasodilation. This included the downregulation of olfactory receptors, acetylcholine channels and hyperaldosteronin/renin pathways, alongside upregulated hypoxia pathways, suggesting deregulation of the vascular tone and blood pressure because of a hypoxic environment.[42]

Additional transcriptional analysis of trophoblast and villous core stromal compartments from SARS-CoV-2-infected samples identified several transcriptional variations that have been previously associated with preeclampsia (Figure 3). Trophoblasts had higher expression of *EGFR*, a marker that increases with hypoxia and is known to upregulate *FLT1*, where excessive release of soluble FLT1 by syncytiotrophoblasts is a characteristic marker of late onset preeclampsia.[43] There was prominent increase of *PAPPA2* in the trophoblasts, the latter considered to become upregulated in response to hypoxia, and placental pathologies, including preeclampsia.[44] Notably, the PAPPA2 substrates IGFBP4 and IGFBP5 were concurrently upregulated in the villous core stromal compartment. The interaction of PAPPA2 with IGFBP4/5 increases levels of IGF2, which was also elevated in the villous core stromal cells in the SARS-CoV-2-infected group (Figure 3d).[34] Additionally, the villous core stromal compartment had decreased levels of Isthmin-2 (*ISM2*), a placental marker that is downregulated with preeclampsia.[45] *GDF15*, *TFPI-2*, *KISS1* and *CRH* genes were also upregulated in SARS-CoV-2-infected trophoblasts, all previously associated with placental oxidative stress, hypertension and preeclampsia.[34,46–48]

In conclusion, our data suggest that the placenta from pregnancies with SARS-CoV-2 adopts a transcriptional profile aligning with placental dysfunction that has been observed in pregnant participants who develop 'preeclampsia-like' syndrome. While further studies on larger cohorts of patients will be required to confirm the outcomes from this study, using digital spatial profiling, our studies showcased the crosstalk between the trophoblast and villous core stromal cell populations, and how this is enriched with pathways associated with placental dysfunction. Our findings set the foundation for a more comprehensive understanding of placental dysfunction in pregnant individuals with SARS-CoV-2 infection and offer important insights into the potential mechanisms through which SARS-CoV-2 may impact pregnancy outcomes and foetal development.

METHODS

Study design

The SARS-CoV-2 group ($n = 7$) consisted of pregnant, unvaccinated participants, who were symptomatic with COVID-19 in their third trimester (confirmed by RT-qPCR from nasopharyngeal swabs). Placental tissue samples were collected at birth at the Hospital de Clínicas (HC) and Hospital Nossa Senhora das Graças, Brazil, with ethics approval from the National Commission for Research Ethics (CONEP) under approval number 30188020.7.1001.0020.[49] The control group was composed of archived placentae from nine COVID19-negative people collected during delivery at the Complexo Hospital de Clínicas, Universidade Federal do Paraná, Curitiba, Brazil between 2016 and 2018. To account for maternal co-morbidities, maternal age and gestational age, the control group was selected to match these clinical features as presented in the SARS-CoV-2 group. Participant cohorts and their clinical characteristics are summarised in Table 1. Morphological analysis was performed in all placentas from SARS-CoV-2-infected and control groups using the Amsterdam Placental Workshop Group Consensus Statement.[50] Histological sections were systematically identified and evaluated by two experienced pathologists to obtain samples for tissue microarray (TMA) construction, as

described in a previous work.[49] Two TMAs were prepared from the placental samples, following the workflow demonstrated in Figure 1.

RNAscope

A serial section from the TMAs (4 μm) was incubated with RNAscope probes targeting SARS-CoV-2 spike mRNA (nCoV2019, #848568-C3, ACDBio, CA, USA), as per manufacturer's instructions for automation on Leica Bond RX. DNA was visualised with Syto13 (500 nM, #S7575, ThermoFisher Scientific, MA, USA), and SARS-CoV-2 spike mRNA with TSA Plus CY5 (1:1500, #NEL745001KT, Akoya Biosciences, MA, USA). Fluorescent images were acquired with NanoString GeoMX DSP at 20×.

Digital spatial profiling with Nanostring GeoMX platform

TMA slides were freshly sectioned (4-μm thick serial sections) and prepared according to the Nanostring GeoMX Digital Spatial Profiler (DSP) slide preparation for RNA profiling (NanoString, WA, USA). Slides were hybridised with the NanoString Technologies Whole Transcriptome Atlas (WTA) barcoded probe set (~18 000 genes), followed by fluorescent staining with Pan-Cytokeratin (PanCK, clone AE-1/AE-3, AF488, Santa Cruz NBP2-33200AF488 [2 μg mL^{-1}], CA, USA) to identify trophoblasts, vimentin (VIM, clone E-5, AF594, Santa Cruz sc-373 717 [1 μg mL^{-1}]) to identify endothelial and mesenchymal stromal cells, and SYTO83 to identify nuclei. With the aid of a trained placental pathologist, an area featuring an anchoring villus, and an area featuring a cluster of terminal villi, were designated as two areas of interest (AOI) within each placental core. Oligonucleotides linked to hybridised mRNA targets were cleaved separately for PanCK positive regions within each AOI, and separately for vimentin positive regions. Cleaved oligonucleotides were collected for counting using Illumina i5 and i7 dual indexing as described previously.[51,52] Paired-end sequencing (2 × 75) was performed using an Illumina NextSeq550 up to 400 M total aligned reads. Fastq files were processed using the Nanostring DND system and uploaded to the GeoMX DSP system where raw counts were aligned with their respective AOIs.

Data normalisation, differential expression analysis and pathway enrichment analysis

Raw data were normalised to the 134 negative probes in the Human Whole Transcriptome Atlas probe set followed by upper quantile normalisation using the R package RUVseq.[53] Transcriptional data from PanCK positive regions within each AOI were normalised separately to the vimentin positive regions. Differential gene expression analysis between SARS-CoV-2 positive and negative groups was performed separately for PanCK positive regions within each AOI, and separately for vimentin positive regions, using the R package limma.[54] The Bayesian adjusted t-statistic method was used where foetal sex and TMA slide number were considered as co-variants. A fold change of ± 1.5 and *P*-value ≤ 0.05 (adjusted for a false discovery rate of 5%) was considered significant. Pathway enrichment analysis was performed using the Gene Set Enrichment Analysis program (GSEA, v4.3.2, Broad Institute, MA, USA) for biological pathways obtained from the Molecular Signatures Database (MSigDB, Broad Institute, Human v2022.1). The preeclampsia gene-set was obtained from Moslehi *et al*.[35] GSEA parameters: 1000 permutations, weighted analysis. Gene set enrichment data were further clustered and visualised using the R package vissE with the parameters: computeMsigOverlap (thresh = 0.25), findMsigClusters (alg = cluster_walktrap, minSize = 2).[55]

ACKNOWLEDGMENTS

This study was funded by the Queensland University of Technology ECR funds for AK, JR, MA, NS. The following authors are supported by fellowships from the NHMRC (AK – 1157741, GB – 2008542 and 1135898) and US Department of Defense (NS – PC190533). The authors thank Fred Hutchinson Pathology (Miki Haraguchi & Stephanie Weaver) for histology assistance. Open access publishing facilitated by The University of Queensland, as part of the Wiley - The University of Queensland agreement via the Council of Australian University Librarians.

AUTHOR CONTRIBUTIONS

Nataly Stylianou: Conceptualization; formal analysis; funding acquisition; investigation; methodology; writing – original draft; writing – review and editing. **Ismail Sebina:** Data curation; formal analysis; investigation; supervision; writing – original draft; writing – review and editing. **Nicholas Matigian:** Formal analysis; investigation; methodology; writing – review and editing. **James Monkman:** Formal analysis; investigation; methodology; writing – review and editing. **Hadeel Doehler:** Writing – review and editing. **Joan Röhl:** Conceptualization; funding acquisition; investigation; methodology; project administration; writing – review and editing. **Mark Allenby:** Conceptualization; funding acquisition; investigation; methodology; writing – review and editing. **Andy Nam:** Formal analysis; investigation; methodology; writing – review and editing. **Liuliu Pan:** Formal analysis; investigation; methodology; writing – review and editing. **Anja Rockstroh:** Formal analysis; investigation; methodology. **Habib Sadeghirad:** Investigation; methodology; writing – review and editing. **Kimberley Chung:** Methodology; writing – review and editing. **Thais Sobanski:** Investigation; methodology; writing – review and editing. **Ken O'Byrne:** Funding acquisition; methodology; writing – review and editing. **Ana Clara Simoes Florido Almedia:** Investigation; methodology; writing – review and editing. **Patricia Zadorosnei Rebutini:** Investigation; methodology. **Cleber Machado-Souza:** Investigation; methodology; writing – review and editing. **Emanuele Therezinha Schueda Stonoga:** Investigation; methodology. **Majid E Warkiani:** Investigation; methodology; writing – review and editing. **Carlos Salomon:** Investigation; methodology; writing – review and editing. **Kirsty Short:** Writing – review and editing. **Lana McClements:** Formal analysis; investigation; methodology; writing – review and editing. **Lucia de Noronha:** Conceptualization; data curation; formal analysis; investigation; methodology; project administration; resources; writing – review and editing. **Ruby Huang:** Conceptualization; formal analysis; investigation; methodology; writing – original draft. **Gabrielle T Belz:**

Investigation; methodology; writing – original draft; writing – review and editing. **Fernando Souza-Fonseca-Guimaraes:** Conceptualization; investigation; methodology; project administration; supervision; writing – review and editing. **Vicki Clifton:** Conceptualization; formal analysis; investigation; methodology; supervision; writing – original draft; writing – review and editing. **Arutha Kulasinghe:** Conceptualization; formal analysis; funding acquisition; investigation; methodology; project administration; supervision; visualization; writing – original draft; writing – review and editing.

CONFLICT OF INTEREST

Andy Nam and Liuliu Pan are employed by Nanostring Technologies. Nicolas Matigian is employed by QCIF Bioinformatics.

DATA AVAILABILITY STATEMENT

The data generated in this study are available in the Gene Expression Omnibus (GEO) under GSE223612.

REFERENCES

1. Bordt EA, Shook LL, Atyeo C *et al*. Maternal SARS-CoV-2 infection elicits sexually dimorphic placental immune responses. *Sci Transl Med* 2021; **13**: eabi7428.
2. Edlow AG, Li JZ, Collier AY *et al*. Assessment of maternal and neonatal SARS-CoV-2 viral load, Transplacental antibody transfer, and placental pathology in pregnancies during the COVID-19 pandemic. *JAMA Netw Open* 2020; **3**: e2030455.
3. Schwartz DA, Mulkey SB, Roberts DJ. SARS-CoV-2 Placentitis, stillbirth and maternal COVID-19 vaccination: Clinical-pathological correlations. *Am J Obstet Gynecol* 2022; **228**: 261–269.
4. Racicot K, Mor G. Risks associated with viral infections during pregnancy. *J Clin Invest* 2017; **127**: 1591–1599.
5. Palomo M, Youssef L, Ramos A *et al*. Differences and similarities in endothelial and angiogenic profiles of preeclampsia and COVID-19 in pregnancy. *Am J Obstet Gynecol* 2022; **227**: 277.e1–277.e16.
6. Mendoza M, Garcia-Ruiz I, Maiz N *et al*. Pre-eclampsia-like syndrome induced by severe COVID-19: A prospective observational study. *BJOG* 2020; **127**: 1374–1380.
7. Serrano B, Bonacina E, Garcia-Ruiz I *et al*. Confirmation of preeclampsia-like syndrome induced by severe COVID-19: An observational study. *Am J Obstet Gynecol MFM* 2022; **5**: 100760.
8. Naeh A, Berezowsky A, Yudin MH, Dhalla IA, Berger H. Preeclampsia-like syndrome in a pregnant patient with coronavirus disease 2019 (COVID-19). *J Obstet Gynaecol Can* 2022; **44**: 193–195.
9. Celewicz A, Celewicz M, Michalczyk M *et al*. SARS CoV-2 infection as a risk factor of preeclampsia and pre-term birth. An interplay between viral infection, pregnancy-specific immune shift and endothelial dysfunction may lead to negative pregnancy outcomes. *Ann Med* 2023; **55**: 2197289.
10. Gonzalez-Vanegas O, Martinez-Perez O. SARS-CoV-2 infection and preeclampsia-how an infection can help us to know more about an obstetric condition. *Viruses* 2023; **15**: 1564.
11. Schwartz DA, Avvad-Portari E, Babál P *et al*. Placental tissue destruction and insufficiency from COVID-19 causes stillbirth and neonatal death from hypoxic-ischemic injury. *Arch Pathol Lab Med* 2022; **146**: 660–676.
12. Huang C, Wang Y, Li X *et al*. Clinical features of patients infected with 2019 novel coronavirus in Wuhan, China. *Lancet* 2020; **395**: 497–506.
13. Maltepe E, Fisher SJ. Placenta: The forgotten organ. *Annu Rev Cell Dev Biol* 2015; **31**: 523–552.
14. Buchrieser J, Degrelle SA, Couderc T *et al*. IFITM proteins inhibit placental syncytiotrophoblast formation and promote fetal demise. *Science* 2019; **365**: 176–180.
15. Wedenoja S, Yoshihara M, Teder H *et al*. Fetal HLA-G mediated immune tolerance and interferon response in preeclampsia. *EBioMedicine* 2020; **59**: 102872.
16. Hamldar S, Kiani SJ, Khoshmirsafa M *et al*. Expression profiling of inflammation-related genes including IFI-16, NOTCH2, CXCL8, THBS1 in COVID-19 patients. *Biologicals* 2022; **80**: 27–34.
17. Kulasinghe A, Tan CW, Ribeiro Dos Santos Miggiolaro AF *et al*. Profiling of lung SARS-CoV-2 and influenza virus infection dissects virus-specific host responses and gene signatures. *Eur Respir J* 2022; **59**: 2101881.
18. Conca W, Alabdely M, Albaiz F *et al*. Serum beta2-microglobulin levels in coronavirus disease 2019 (Covid-19): Another prognosticator of disease severity? *PloS One* 2021; **16**: e0247758.
19. Jain NK, Tailang M, Jain HK *et al*. Therapeutic implications of current Janus kinase inhibitors as anti-COVID agents: A review. *Front Pharmacol* 2023; **14**: 1135145.
20. Hu XQ, Zhang L. Hypoxia and mitochondrial dysfunction in pregnancy complications. *Antioxidants (Basel)* 2021; **10**: 405.
21. Rana S, Burke SD, Karumanchi SA. Imbalances in circulating angiogenic factors in the pathophysiology of preeclampsia and related disorders. *Am J Obstet Gynecol* 2022; **226**: S1019–S1034.
22. Mukosera GT, Clark TC, Ngo L *et al*. Nitric oxide metabolism in the human placenta during aberrant maternal inflammation. *J Physiol* 2020; **598**: 2223–2241.
23. Van Hove CE, Van der Donckt C, Herman AG, Bult H, Fransen P. Vasodilator efficacy of nitric oxide depends on mechanisms of intracellular calcium mobilization in mouse aortic smooth muscle cells. *Br J Pharmacol* 2009; **158**: 920–930.
24. Jansson T, Aye IL, Goberdhan DC. The emerging role of mTORC1 signaling in placental nutrient-sensing. *Placenta* 2012; **33**(Suppl 2): e23–e29.
25. Hastie R, Brownfoot FC, Pritchard N *et al*. EGFR (epidermal growth factor receptor) signaling and the mitochondria regulate sFlt-1 (soluble FMS-like tyrosine Kinase-1) secretion. *Hypertension* 2019; **73**: 659–670.
26. Kramer AW, Lamale-Smith LM, Winn VD. Differential expression of human placental PAPP-A2 over gestation and in preeclampsia. *Placenta* 2016; **37**: 19–25.
27. Neuman RI, Alblas van der Meer MM, Nieboer D *et al*. PAPP-A2 and inhibin a as novel predictors for pregnancy complications in women with suspected or confirmed preeclampsia. *J Am Heart Assoc* 2020; **9**: e018219.
28. Lamale-Smith LM, Gumina DL, Kramer AW *et al*. Uteroplacental ischemia is associated with increased PAPP-A2. *Reprod Sci* 2020; **27**: 529–536.

29. Guerby P, Tasta O, Swiader A *et al*. Role of oxidative stress in the dysfunction of the placental endothelial nitric oxide synthase in preeclampsia. *Redox Biol* 2021; **40**: 101861.
30. Karteris E, Vatish M, Hillhouse EW, Grammatopoulos DK. Preeclampsia is associated with impaired regulation of the placental nitric oxide-cyclic guanosine monophosphate pathway by corticotropin-releasing hormone (CRH) and CRH-related peptides. *J Clin Endocrinol Metab* 2005; **90**: 3680–3687.
31. Ibanoglu MC, Oskovi-Kaplan ZA, Ozgu-Erdinc AS, Kara O, Sahin D. Comparison of the Kisspeptin levels in early onset preeclampsia and late-onset preeclampsia. *Arch Gynecol Obstet* 2022; **306**: 991–996.
32. Cruickshank T, MacDonald TM, Walker SP *et al*. Circulating growth differentiation factor 15 is increased preceding preeclampsia diagnosis: Implications as a disease biomarker. *J Am Heart Assoc* 2021; **10**: e020302.
33. Kobayashi H, Matsubara S, Yoshimoto C, Shigetomi H, Imanaka S. Tissue factor pathway inhibitors as potential targets for understanding the pathophysiology of preeclampsia. *Biomedicine* 2023; **11**: 1237.
34. Nishizawa H, Pryor-Koishi K, Suzuki M *et al*. Increased levels of pregnancy-associated plasma protein-A2 in the serum of pre-eclamptic patients. *Mol Hum Reprod* 2008; **14**: 595–602.
35. Moslehi R, Mills JL, Signore C, Kumar A, Ambroggio X, Dzutsev A. Integrative transcriptome analysis reveals dysregulation of canonical cancer molecular pathways in placenta leading to preeclampsia. *Sci Rep* 2013; **3**: 2407.
36. Aouache R, Biquard L, Vaiman D, Miralles F. Oxidative stress in preeclampsia and placental diseases. *Int J Mol Sci* 2018; **19**: 1496.
37. Redman CW, Staff AC. Preeclampsia, biomarkers, syncytiotrophoblast stress, and placental capacity. *Am J Obstet Gynecol* 2015; **213**: S9 e1. S9-11.
38. Mistry HD, Czajka AN, Kurlak LO, Pipkin FB, Taggart MJ, Tribe RT. Differential placental caveolin-1 gene expression in women with pre-eclampsia. *Arch Dis Child Fetal Neonatal Edn* 2011; **96**: Fa125–Fa126.
39. Nowicki B, Singhal J, Fang L, Nowicki S, Yallampalli C. Inverse relationship between severity of experimental pyelonephritis and nitric oxide production in C3H/HeJ mice. *Infect Immun* 1999; **67**: 2421–2427.
40. Ogando DG, Paz D, Cella M, Franchi AM. The fundamental role of increased production of nitric oxide in lipopolysaccharide-induced embryonic resorption in mice. *Reproduction* 2003; **125**: 95–110.
41. Kong L, Zhang Q, Chao J *et al*. Polarization of macrophages induced by toxoplasma gondii and its impact on abnormal pregnancy in rats. *Acta Trop* 2015; **143**: 1–7.
42. Wareing M, Bai X, Seghier F *et al*. Expression and function of potassium channels in the human placental vasculature. *Am J Physiol Regul Integr Comp Physiol* 2006; **291**: R437–R446.
43. Roberts JM, Rich-Edwards JW, McElrath TF, Garmire L, Myatt L, Global Pregnancy C. Subtypes of preeclampsia: Recognition and determining clinical usefulness. *Hypertension* 2021; **77**: 1430–1441.
44. Wagner PK, Otomo A, Christians JK. Regulation of pregnancy-associated plasma protein A2 (PAPPA2) in a human placental trophoblast cell line (BeWo). *Reprod Biol Endocrinol* 2011; **9**: 48.
45. Martinez C, Gonzalez-Ramirez J, Marin ME *et al*. Isthmin 2 is decreased in preeclampsia and highly expressed in choriocarcinoma. *Heliyon* 2020; **6**: e05096.
46. Sugulle M, Dechend R, Herse F *et al*. Circulating and placental growth-differentiation factor 15 in preeclampsia and in pregnancy complicated by diabetes mellitus. *Hypertension* 2009; **54**: 106–112.
47. Hogg K, Blair JD, McFadden DE, von Dadelszen P, Robinson WP. Early onset pre-eclampsia is associated with altered DNA methylation of cortisol-signalling and steroidogenic genes in the placenta. *PloS One* 2013; **8**: e62969.
48. Zheng L, Huang J, Su Y, Wang F, Kong H, Xin H. Overexpression of tissue factor pathway inhibitor 2 attenuates trophoblast proliferation and invasion in preeclampsia. *Hum Cell* 2020; **33**: 512–520.
49. Rebutini PZ, Zanchettin AC, Stonoga ETS *et al*. Association between COVID-19 pregnant women symptoms severity and placental morphologic features. *Front Immunol* 2021; **12**: 685919.
50. Khong TY, Mooney EE, Ariel I *et al*. Sampling and definitions of placental lesions: Amsterdam placental workshop group consensus statement. *Arch Pathol Lab Med* 2016; **140**: 698–713.
51. Merritt CR, Ong GT, Church SE *et al*. Multiplex digital spatial profiling of proteins and RNA in fixed tissue. *Nat Biotechnol* 2020; **38**: 586–599.
52. Jerby-Arnon L, Neftel C, Shore ME *et al*. Opposing immune and genetic mechanisms shape oncogenic programs in synovial sarcoma. *Nat Med* 2021; **27**: 289–300.
53. Risso D, Ngai J, Speed TP, Dudoit S. Normalization of RNA-seq data using factor analysis of control genes or samples. *Nat Biotechnol* 2014; **32**: 896–902.
54. Ritchie ME, Phipson B, Wu D *et al*. Limma powers differential expression analyses for RNA-sequencing and microarray studies. *Nucleic Acids Res* 2015; **43**: e47.
55. Dharmesh D, Bhuva CWT, Ning L *et al*. vissE: A versatile tool to identify and visualise higher-order molecular phenotypes from functional enrichment analysis. *bioRxiv* 2022. https://doi.org/10.1101/2022.1103.1106.483195

Supporting Information

Additional supporting information may be found online in the Supporting Information section at the end of the article.